

# Colour gradients of low-redshift galaxies in the DESI Legacy Imaging Survey

Li-Wen Liao<sup>1,2</sup>  and Andrew P. Cooper<sup>1,2,3</sup>

<sup>1</sup>Institute of Astronomy and Department of Physics, National Tsing Hua University, Hsinchu 30013, Taiwan

<sup>2</sup>Center for Informatics and Computation in Astronomy, National Tsing Hua University, Hsinchu 30013, Taiwan

<sup>3</sup>Physics Division, National Center for Theoretical Sciences, Taipei 10617, Taiwan

**Abstract.** Radial colour gradients within galaxies arise from gradients of stellar age, metallicity, and dust reddening. Large samples of colour gradients from wide-area imaging surveys can be used to constrain galaxy formation models. Here we measured colour gradients for low-redshift galaxies using photometry from the 9<sup>th</sup> DESI Legacy Imaging Survey (LS), which reaches  $r \sim 24$  over  $\sim 14,000 \text{ deg}^2$ . We investigate empirical relationships between colour gradients,  $M_*$ , and sSFR. We compared our results with the prediction of the Illustris TNG-100 simulation using SDSS mock images.

**Keywords.** galaxies: formation, galaxies: statistics, galaxies: structure, galaxies: general

## 1. Introduction

Radial colour gradients in galaxies arise from age and metallicity gradients (Tinsley & Larson 1978). These gradients are closely related to the distribution of the stellar population, which is influenced by galaxy assembly history and formation processes. Therefore, colour gradients are expected to vary with observational parameters, such as colour, mass, and sSFR (e.g., de Jong 1996; Tortora et al. 2010). For example, late-type galaxies are expected to grow ‘inside out’ through gradual gas accretion, leading to the result that old stars centralise at a centre region of galaxies and producing a negative colour gradient. For early-type galaxies major mergers could redistribute the stellar component and result in relatively flat colour gradients.

In our work, we used the 9<sup>th</sup> data release from the DESI Legacy Imaging Survey (Dey et al. 2019), which has a coverage of  $\sim 14,000 \text{ deg}^2$  and provides catalogues containing effective radius ( $R_{\text{eff}}$ ), and fluxes within circular apertures with radii [0.5, 0.75, 1.0, 1.5, 2.0, 3.5, 5.0, 7.0] arcsec around each source. We plot surface brightness profiles and colour profiles computed from these aperture fluxes. Colour gradients are defined as  $\nabla_{X-Y} = \delta(X - Y) / \delta(R/R_{\text{eff}})$ , the slope of  $X - Y$  colour versus  $R/R_{\text{eff}}$ . We choose  $R_1 = 0.5R_{\text{eff}}$  and  $R_2 = R_{\text{eff}}$ . Galaxies will have a negative colour gradient if their central region is more red than their outer part. Galaxies will have a negative colour gradient. The spectroscopic redshifts of galaxies are obtained from the SDSS. Details about sample selection can be found in Liao & Cooper (2022).

## 2. Colour gradient as a function of $M_*$ and sSFR

Fig. 1 shows  $g - r$  colour gradients ( $\nabla_{g-r}$ ) versus stellar mass ( $M_*$ ) and specific star formation rate (sSFR). We divided galaxies into red and blue using a colour magnitude

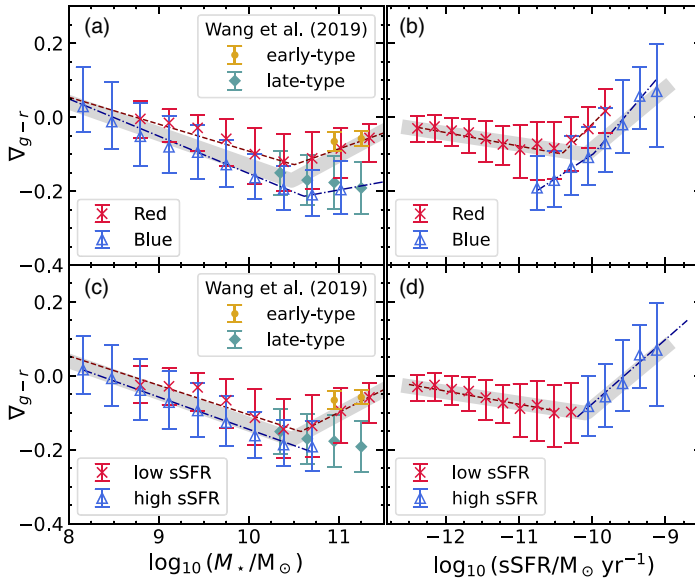


**Figure 1.** Colour gradients as a function of  $M_*$  and sSFR for red/blue galaxies (upper panels) and high-/low-sSFR galaxies (lower panels). The error bars indicate the 25-75 percentile range. The solid diamond and dots show colour gradients computed from the Wang et al. (2019).

diagram, and high-sSFR and low-sSFR galaxies using their sSFRs. The results show that the colour gradients of galaxies with  $M_*$  less than  $10^{10.5} M_\odot$  decrease (become steeper) as the stellar mass increases. This colour gradient trend holds for red/blue and high-sSFR/low-sSFR galaxies, suggesting that galaxies may undergo a similar formation process in this regime. One broadly accepted scenario is the “inside-out” formation scenario, in which galaxies form gradually as gas is accreted and cooled in growing dark matter halos (Larson 1974; De Lucia & Blaizot 2007). The oldest stars are located at the centres of galaxies, in the earliest-forming and deepest part of the gravitational potential. In contrast, younger stars are formed with lower binding energy, with the support of angular momentum. This age difference creates negative colour gradients.

For galaxies with  $M_* > 10^{10.5} M_\odot$ , colour gradients are flatter with increasing mass, especially for red/low-sSFR galaxies. The inflection of colour gradient trends around  $M_* \sim 10^{10.5} M_\odot$  coincides with a critical host halo virial mass, above which the AGN feedback is thought to dominate for galaxies massive (Kauffmann et al. 1996; Guo & White 2008). The suppression of the halo cooling flow by AGN reduces the star-formation rate of galaxies (quenching). Therefore, for galaxies above the transition mass, major mergers drive their subsequent stellar mass growth. During major mergers, the stellar components can be redistributed through violent relaxation, resulting in colour gradients that flatten with successive generations of merging. An alternative explanation for the flattening trends of colour gradient to high mass is that, in a passively evolving galaxy, a fixed age gradient results in a flatter colour gradient for larger absolute age, because younger populations redden more rapidly.

### 3. Comparison to Illustris TNG100

The Next Generation Illustris Simulation, IllustrisTNG, is a suite of cosmological megnetohydrodynamic simulations (Pillepich et al. 2018; Springel et al. 2018; Nelson et al. 2018; Naiman et al. 2018; Marinacci et al. 2018). To compare our results with these simulations, we measured the colour gradients of galaxies with mock SDSS *griz* images

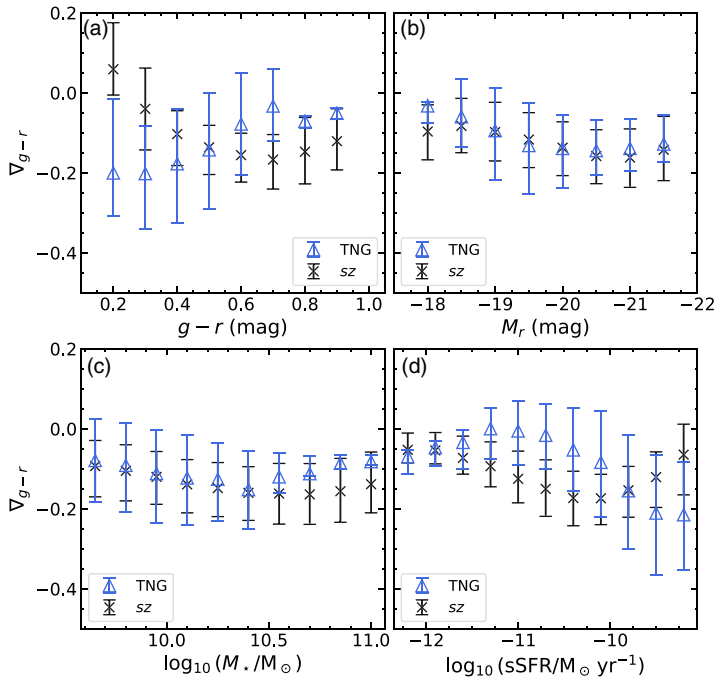


**Figure 2.**  $\nabla_{g-r}$  for TNG100 (triangles) and out mass-limited sample (crosses) as a function of (a)  $g-r$ , (b)  $M_r$ , (c)  $M_*$ , and (d) sSFR. The error bar label 25<sup>th</sup> and 75<sup>th</sup> percentile.

in the dataset provided by [Rodriguez-Gomez et al. \(2017\)](#). In Fig. 2, we plot the colour gradients of galaxies in IllustrisTNG as a function of  $g-r$ ,  $M_r$ ,  $M_*$  and sSFR. The trends of  $g-r$  and sSFR are very different to the observational results. There may be many reasons for these differences; we speculate that the discrepancy could be mitigated by a decrease in the late-time sSFR of TNG galaxies. In contrast to  $g-r$  and sSFR, the trends of  $M_r$  and  $M_*$  agree well with the observations, especially for low-mass galaxies. The results support the model of supernova feedback in TNG.

## References

- De Lucia G., Blaizot J., 2007, [MNRAS](#), **375**, 2
- Dey A., et al., 2019, [AJ](#), **157**, 168
- Guo Q., White S. D. M., 2008, [MNRAS](#), **384**, 2
- Kauffmann G., Charlot S., White S. D. M., 1996, [MNRAS](#), **283**, L117
- Larson R. B., 1974, [MNRAS](#), **166**, 585
- Liao L.-W., Cooper A., 2022, arXiv e-prints, p. [arXiv:2209.14166](#)
- Marinacci F., et al., 2018, [MNRAS](#), **480**, 5113
- Naiman J. P., et al., 2018, [MNRAS](#), **477**, 1206
- Nelson D., et al., 2018, [MNRAS](#), **475**, 624
- Pillepich A., et al., 2018, [MNRAS](#), **475**, 648
- Rodriguez-Gomez V., et al., 2017, [MNRAS](#), **467**, 3083
- Springel V., et al., 2018, [MNRAS](#), **475**, 676
- Tinsley B. M., Larson R. B., 1978, [ApJ](#), **221**, 554
- Tortora C., Napolitano N. R., Cardone V. F., Capaccioli M., Jetzer P., Molinaro R., 2010, [MNRAS](#), **407**, 144
- Wang W., et al., 2019, [MNRAS](#), **487**, 1580
- de Jong R. S., 1996, in Minniti D., Rix H.-W., eds, *Spiral Galaxies in the Near-IR*. p. 43 ([arXiv:astro-ph/9509001](#)), doi:10.1007/978-3-540-49739-4\_6